Thin Solid Films 633 (2017) 151–155

Contents lists available at ScienceDirect

Thin Solid Films

journal homepage: www.elsevier.com/locate/tsf

An innovative approach for fabrication of $Cu_2ZnSnSe_4$ absorber layers using solutions of elemental metal powders

Carl S. Cooper [a,b,*], Panagiota Arnou [b], Lewis D. Wright [b], Soňa Uličná [b], John M. Walls [b], Andrei V. Malkov [a,c], Jake W. Bowers [b,**]

[a] Department of Chemistry, Loughborough University, Loughborough, Leicestershire LE11 3TU, UK
[b] Centre for Renewable Energy Systems Technology (CREST), Wolfson School of Mechanical, Electrical and Manufacturing Engineering, Loughborough University, Loughborough, Leicestershire LE11 3TU, UK
[c] Department of Chemistry, RUDN, 6 Miklukho-Maklaya Street, Moscow 117198, Russia

ARTICLE INFO

Article history:
Received 18 May 2016
Received in revised form 14 December 2016
Accepted 16 December 2016
Available online 18 December 2016

Keywords:
Copper zinc tin selenide
Solution process
Spray-coating
Kesterite

ABSTRACT

An innovative approach has been demonstrated for the deposition of $Cu_2ZnSnSe_4$ (CZTSe) absorber layers. Using a unique, safe solvent combination, moving away from hydrazine, elemental Cu, Zn, Sn and S/Se can be fully dissolved at ambient conditions, with the composition easily controlled. The preparation and the spray deposition of these solutions are performed in air, allowing a quick, easy and inexpensive process. Upon selenisation, large crystals are observed which are identified as the CZTSe kesterite phase using X-ray diffraction and Raman, the latter showing no distinctive signs of any binary or ternary secondary phases. Using this method, CZTSe absorber layers have been prepared for use in thin-film solar cells reaching efficiency of 3.2%. With further device optimisation, improved device performance will be achieved.

1. Introduction

$Cu_2ZnSn(S,Se)_4$ (CZTSSe) compounds have emerged as an ideal replacement for current thin-film technology (such as CdTe or CIGS), due to their suitable band gap and high absorption coefficient, in addition to incorporating less toxic and more earth-abundant materials. However, improvements in efficiency are required before CZTSSe becomes a viable replacement.

There are numerous methods to prepare CZTSSe thin-films, including but not limited to: sputtering, co-evaporation, electrodeposition and several solution-processed methods [1]. This study will look into the method reported by Mitzi et al. [2], where the required elements are directly dissolved, without the use of salts which may incorporate detrimental impurities in the film. After depositing, the absorber layers are intermediately dried and the solvents decompose cleanly, forming a CZTSSe layer that is free from impurities. Direct solution processing is an ideal way to prepare CZTSSe, as the composition can be controlled easily, allowing band gap control. CZTSSe thin films can be deposited by many techniques including doctor blading, spin coating and spray coating. These techniques can be used to deposit the samples quickly, without the requirement of high vacuum equipment. However, solution processing of elemental metals and chalcogenides is typically challenging, due to their insolubility in most common solvents.

There have only been a few solvents that were implemented in the direct solution processing of CZTS absorber layers using elemental metals or chalcogenides. Mitzi et al. dissolved metal chalcogenides in hydrazine, for depositing CIGS [3] and later CZTSSe [2]. The solutions were deposited by spin coating and hydrazine was removed with a short drying step, leaving a uniform layer of CIGS and CZTS. Whilst the method proposed by Mitzi et al. [2,3] is effective, hydrazine is highly toxic and explosive, making the process hard to scale up. Therefore, an ideal approach should follow the main principles described by Mitzi [2,3], but using an alternative solvent to hydrazine. The alternative solvent needs to be more environmentally friendly than hydrazine and also should be able to dissolve metal chalcogenides and/or metals and then decompose easily forming a clean absorber layer.

A combination of 1,2-ethanedithiol and ethylenediamine was shown by Webber and Brutchey to dissolve a series of metal sulphides including As_2S_3, Sb_2S_3 and Bi_2S_3 along with their selenide and telluride counterparts [4]. It was shown that phase-pure materials could be obtained after an annealing step at 350 °C. The same group has also developed other methods which could be used for fabrication of thin-film photovoltaics. These include the deposition of SnS [5,6], dissolution of selenium and tellurium [7], amongst others [8].

Previous work by our group demonstrated that Cu_2S, In_2S_3 and their selenide counterparts can be dissolved in the 1,2-ethanedithiol/

* Corresponding author at: Department of Chemistry, Loughborough University, Loughborough, Leicestershire LE11 3TU, UK.
** Corresponding author.
E-mail addresses: C.Cooper2@lboro.ac.uk (C.S. Cooper), J.W.Bowers@lboro.ac.uk (J.W. Bowers).

http://dx.doi.org/10.1016/j.tsf.2016.12.026

ethylenediamine solvent combination [9]. The 1,2-ethanedithiol/ethylenediamine solvent combination was later used for the deposition of $CuInSe_2$ solar cells reaching an efficiency of 8.0% [10]. The solvent combination was later shown by Zhao et al. [11] and Guo et al. [12] to dissolve elemental powders of metals for CIGS and CZTSSe deposition, reaching efficiencies of 9.5% and 6.4%, respectively. Furthermore, a move away from these two solvents was started by Yang et al. [13] using a mixture of thioglycolic acid and ethanolamine to prepare CZTSe precursor solutions, reaching an efficiency of 8.0%. Despite being a better alternative than hydrazine, ethylenediamine and 1,2-ethanedithiol are still relatively toxic solvents, with the dithiol having a strong odor. As these solvents are still not ideal for large scale, there is still a need to find an alternative solvent combination.

In this work, we report an alternative solvent combination of cysteamine and ethanolamine, which has shown to be a suitable replacement. Here, cysteamine is used as the thiol source, and as a solid, it is easier and safer to handle, as well as being significantly less odorous than liquid thiol sources. Cu, Zn, Sn and Se powders have been dissolved in this solvent combination, and the solutions were deposited by a simple chromatography atomiser. After selenising in a graphite box, a crystalline layer of CZTSe was formed. With this method, an efficiency of 3.2% has been reached. Promising results were obtained from the first selenisation trials and show that improvements can be made through device processing optimisation.

2. Experimental details

2.1. Preparation of CZTSe precursor solution

CZTSe solutions were prepared using elemental metal powders. To prepare a solution with ratios of $Cu/(Zn + Sn) = 0.8$ and $Zn/Sn = 1.2$, 1.76 mmol of Cu, 1.00 mmol of Sn, 1.20 mmol of Zn and 4.00 mmol of Se were added to a vial containing 1 g of cysteamine and 10 ml of ethanolamine, which corresponds to an ~10:1 amine/thiol ratio by weight. The mixture was magnetically stirred at room temperature for at least 24 h to allow the metals to fully dissolve and then diluted with dimethyl sulphoxide (DMSO) in a 1:1 ratio before deposition. The metals have been shown to be better soluble in an ~10:1 mixture of amine source to thiol source [4] and therefore this ratio was utilised in the current study. Different thiol/amine ratios were found to show poor dissolution of the metals.

2.2. Absorber formation

The solution was sprayed using a chromatography atomiser onto a preheated molybdenum-coated soda lime glass (SLG) substrate at 310 °C. After each deposited layer, the film was left for 2 min to dry at the same temperature. The temperature of 310 °C was chosen as a balance between removing the solvents and preventing oxidation of the underlying Mo substrate. This method was repeated until the desired thickness was reached, with 6 layers giving an average thickness of 2.0 μm.

After the sample was deposited and dried, a selenisation step was carried out to promote grain growth within the absorber layer. The samples were placed inside a graphite box with ~160 mg of selenium pellets, which was placed in a tube furnace and heated to ~570 °C. Although the temperature set point was 570 °C, the maximum temperature reached, measured by a thermocouple placed under the sample, was 555 °C. The mass of the Se used was determined through preliminary experiments, as too much Se lead to excessive delamination of the film, whilst using less lead to insufficient recrystallisation. The tube furnace was sealed and the graphite box was kept under a nitrogen atmosphere with an initial pressure of 40 kPa, and varied selenisation duration.

2.3. Fabrication of CZTSe device

After selenisation, an ~70 nm cadmium sulphide (CdS) layer was deposited by chemical bath deposition, followed by an ~80 nm intrinsic zinc oxide (i-ZnO) and ~500 nm aluminium doped zinc oxide (AZO) layer, deposited by RF sputtering. Finally, the samples were scribed to give an active area of ~0.25 cm^2.

2.4. Characterisation

The thickness of the absorber layer was measured using a surface profilometer by Ambios (model XP-2). The compositional analyses of the CZTSe thin films was performed using a Bruker Quantax 70 energy dispersive X-ray spectroscopy (EDS), built into a Hitachi TM3030 table top scanning electron microscope (SEM). To analyse the crystallinity of the deposited CZTSe absorber layer, X-ray diffraction (XRD) patterns were taken, using a D2 phaser X-ray diffractometer by Bruker. The X-ray diffractometer was equipped with a Cu-Kα X-ray source and a lynxeye detector. The anti-scatter slit was set at 3 mm and the divergence slit was set at 1 mm. The sample was rotated at 15 rpm. A LabRam HR by Horiba Jobin-Yvon was used for Raman spectroscopy analysis of the samples, using an excitation laser with a wavelength of 633 nm. The high resolution surface and cross-sectional images were obtained using a JEOL 7800F field emission gun scanning electron microscope (FEGSEM). The aperture size was 30 μm with an operating voltage of 5 kV. Photocurrent density – voltage (J-V) curves were recorded under the standard AM1.5 illumination (100 mW cm^{-2}) with a Keithley 2440 5 A source meter.

3. Results and discussion

3.1. Characterisation of the CZTSe absorber layer

The following results were obtained using the starting solution with a $Cu/(Zn + Sn)$ of 0.8 and Zn/Sn ratio of 1.2. The composition can be easily changed to control the final stoichiometry of the CZTSe absorber layer by simply altering the starting concentration of elemental metals. The solutions prepared are optically transparent and remain stable for months (Fig. 1). From EDS analysis, the as-deposited samples gave composition ratios of $Cu/(Zn + Sn) = 0.77–0.88$ and $Zn/Sn = 1.15–1.29$. Notably there is S present in the as-deposited film with a Se/S ratio of ~3.5. The remaining S that is present in the solution comes from the solid cysteamine and the diluting solvent DMSO, showing that S is introduced via the solvent and is still present in the film after drying at 310 °C. However, after selenisation the Se/S ratio increased to ~36.5,

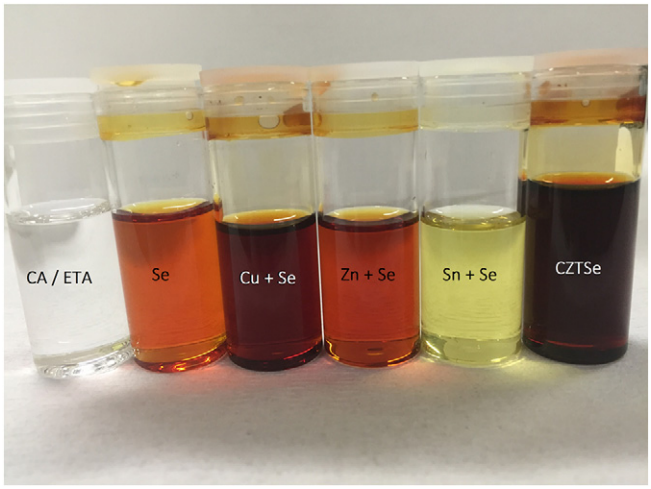

Fig. 1. Varying solutions of metals dissolved in cysteamine and ethanolamine.

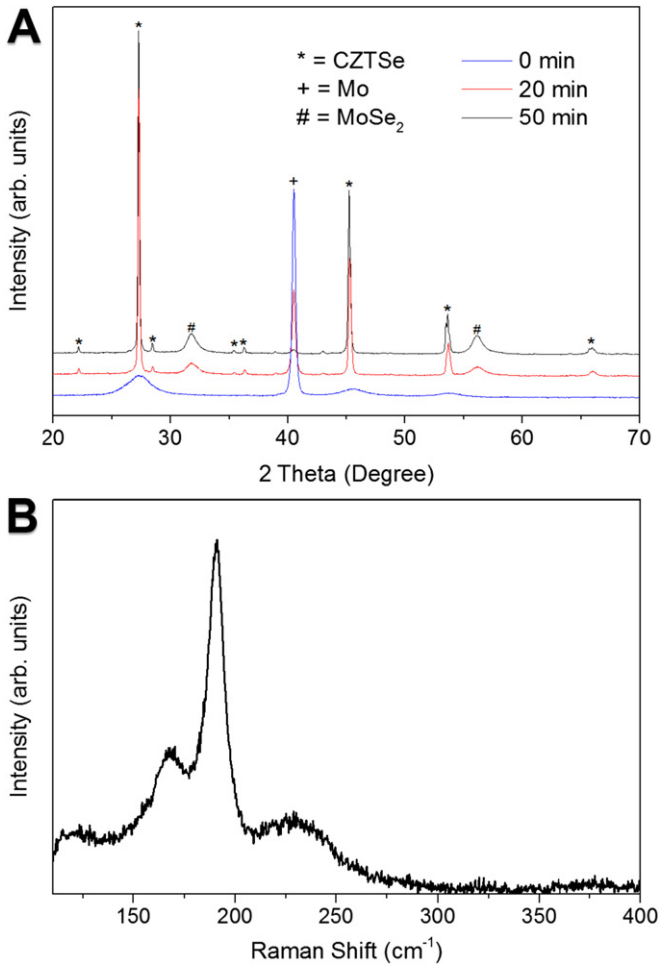

Fig. 2. A) XRD patterns of samples after the selenisation process from 0 to 50 min. B) Raman spectrum of a selenised CZTSe thin-film.

showing that during the selenisation process S is quite significantly displaced by Se.

To identify the growth process of the CZTSe films, XRD measurements were performed for films selenised for 10 to 50 min (Fig. 2 A). The whole process took 26 min to reach the maximum substrate temperature of 555 °C, therefore selenising for 30, 40, and 50 min corresponds to a 4, 14 and 24 min dwell time at the desired temperature, respectively. In the as-deposited films (hence, 0 min selenisation), three broad peaks can be observed, that are associated with the CZTSe structure (JCPDS No. 52-0868), (112) at 27.16°, (220) at 45.12° and (312) at 53.39°. In addition, the XRD pattern of the as-deposited film shows unreacted Mo (110) at 40.63° 2θ (JCPDS No. 42-1120). For a selenisation process of 20 min, where the temperature had only reached 550 °C, the (112), (220) and (312) peaks associated with CZTSe had sharpened. The full width half maximum (FWHM) decreased from 2.20° at 0 min compared to 0.155° after 20 min, showing a significant crystallisation occurring between 10 and 20 min. As the dwell time increased further, the FWHM decreased slowly showing a slight improvement in crystallisation. Moreover, notably, two broad peaks associated with $MoSe_2$, (100) at 31.85° 2θ and (110) at 56.15° 2θ (JCPDS No. 29-0914, 77-1715, 87-2419) can be observed as the Mo (110) signal decreases, which disappears after 30 min of selenisation. This indicates that with these selenisation conditions, Se easily diffuses to the back surface through the porous deposited film.

Raman spectroscopy (Fig. 2B) was performed to distinguish between potential binary and ternary secondary phases, such as Cu_xSe, ZnSe and Cu_2SnSe_3, which may be present when preparing CZTSe. Three distinctive peaks can be observed at wavelengths 170 cm^{-1}, 192 cm^{-1} and 232 cm^{-1} which can be assigned to the CZTSe kesterite phase. There are no observed peaks at 180 cm^{-1}, 253 cm^{-1} and 260 cm^{-1}, respectively for Cu_2SnSe_3, ZnSe and CuSe [14].

3.2. Film morphology

The film morphology was investigated using SEM imaging (Fig. 3). From the surface image, crystals cover the entire surface with no visible cracks or voids. The surface is, however, wavy causing slight variations

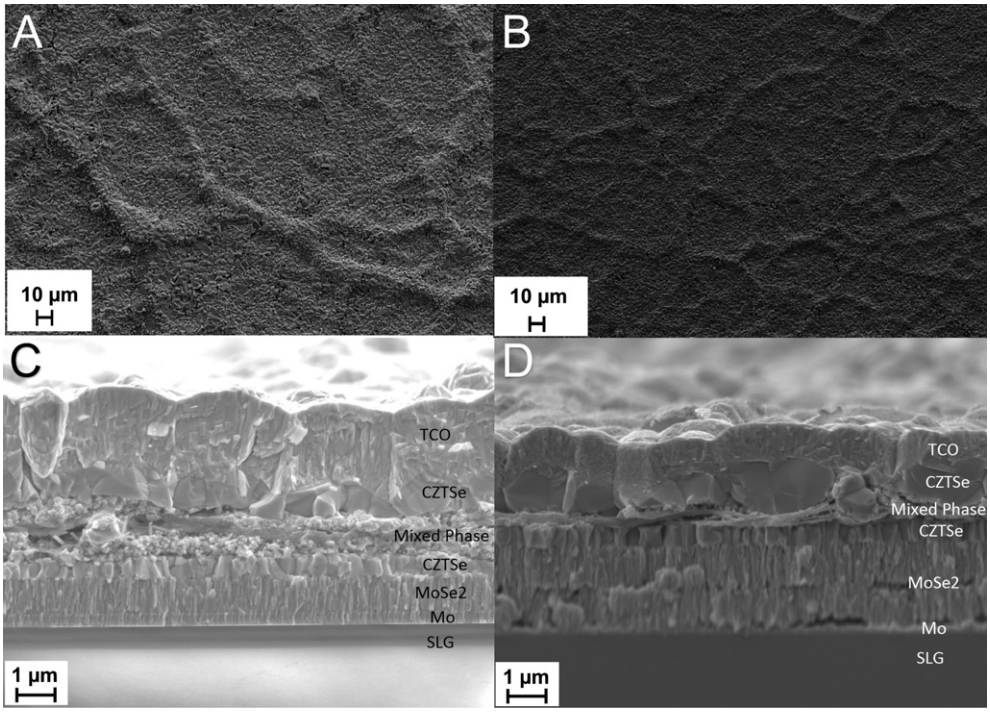

Fig. 3. A) SEM surface image after a 20 min selenisation (2 k× magnification). B) SEM surface image after a 50 min selenisation (1 k× magnification). C) SEM cross-sectional image after a 20 min selenisation. D) SEM cross-sectional image after a 50 min selenisation.

Table 1
Devices prepared using varying selenisation times showing their average Voc, Jsc, FF and efficiency.

Selenisation time (minutes)	Voc (mV)	Jsc (mA·cm^{-2})	FF (%)	Efficiency (%)
20	241 ± 19	23.3 ± 2.0	37 ± 3	2.10 ± 0.42
30	219 ± 15	20.3 ± 1.5	32 ± 1	1.44 ± 0.24
40	211 ± 17	22.3 ± 3.5	31 ± 2	1.47 ± 0.31
50	209 ± 19	16.6 ± 1.8	28 ± 1	0.97 ± 0.18

in thickness throughout the absorber layer, which can be explained by the volume contraction of the solvent upon evaporation during deposition. The deposition process needs further investigation to improve the surface morphology. This may be achieved by optimising the drying temperature, drying time and absorber layer thickness.

Cross-sectional images show three distinctive layers for a 50 min selenisation step, from bottom to top: (1) $MoSe_2$ with a thickness of ~2.0 μm; (2) a "sandwiched" structured absorber layer of ~2.0 μm consisting of ~0.5 μm crystals growing from the bottom and ~1.2 μm growing typically top down, sandwiching ~0.3 μm of uncrystallised absorber layer; (3) CdS, i-ZnO and AZO to complete the device. After 20 min of selenisation the top down crystals were ~0.7 μm with a 1.0 μm of uncrystallised absorber layer. The thick layer of $MoSe_2$ has been shown to have a significant effect on device performance, with increasing thickness of $MoSe_2$ increasing the series resistance of the device [15]. The $MoSe_2$ thickness can be controlled by altering the selenisation conditions or by introducing a barrier layer between the absorber layer and the Mo [15]. Furthermore, it has been reported previously that the "sandwiched" absorber layer is likely formed due to the high porosity of the absorber layer. This allows Se vapour to rapidly diffuse to the bottom and allows crystal growth from the bottom-up [16]. This could also explain why the Mo selenises significantly at a similar time to the crystal growth from the top, as shown by XRD. To solve this problem, a solution soaking step in a cation precursor solution was implemented before selenisation to reduce the porosity of the film [16]. However, with these underlying problems, reasonable efficiencies are still producible, as discussed in Section 3.3.

3.3. J-V analysis

Devices have been prepared and measured with a notable improvement in performance with shorter selenisation times. From comparing the average device parameters prepared after different selenisation times (Table 1), a noticeable drop in all parameters can be observed with increasing selenisation time. Although better crystal growth and a thinner uncrystallised layer are obtained after longer selenisation times, the shortest selenisation time (20 min) resulted in the cell with the highest efficiency of 3.2% (Fig. 4). After 20 min, the selenisation temperature reached only 550 °C for a very short period, before the furnace was turned off and allowed to cool naturally. This improvement with a relatively short selenisation time may be related to thinner $MoSe_2$ forming during shorter selenisations, or excess Sn loss during the prolonged annealing process. Sn loss can lead to formation of Cu and Zn binary phases, causing a deterioration in the series resistance and in turn the efficiency [17]. Further work will be carried out to clarify the reasons for this loss in performance.

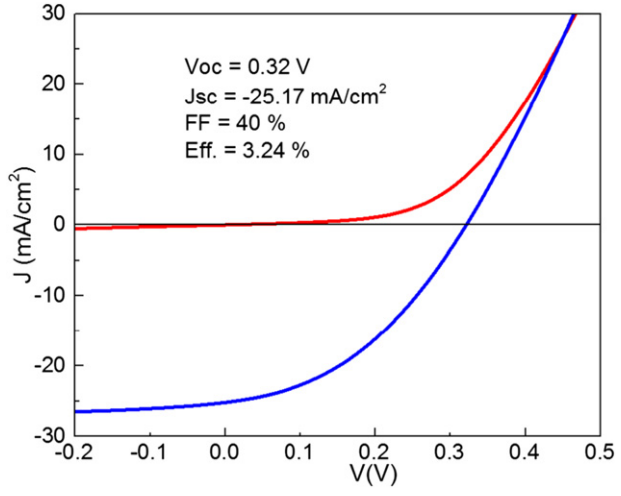

Fig. 4. J-V curve of the best efficiency device (3.2% efficiency) after 20 min selenisation. Whilst the set point temperature was 570 °C, the substrate reached only 550 °C within 20 min.

4. Conclusion

A safe and simple approach has been demonstrated to dissolve elemental powders of metals at room temperature which have several months of shelf life. The metal composition can easily be altered to control the final composition of the film. Spray coating was chosen as a quick method to deposit a thin film of CZTSe precursor, and after selenisation a highly crystalline CZTSe absorber layer was formed, with a device efficiency of 3.2%. Optimisation of individual processes within this method can lead to further improvements in device performance. Improvements in the Mo-coated SLG, deposition and selenisation process can lead to a thinner $MoSe_2$ layer, for example by using a barrier layer [15]. Crystallisation may be improved by further optimisation of the selenisation parameters which include temperature, pressure and Se mass. Finally, the band gap for the current devices was previously calculated to be ~1.0 eV. The incorporation of sulphur into the initial solution and the absorber layer is anticipated to lead to a more favourable band gap.

Acknowledgements

The authors would like to acknowledge Loughborough Materials Characterisation Centre (LMCC) for the use of their facilities for FEGSEM images, as well as the EPSRC PVTEAM project (EP/L017792/1) for funding this work.

References

[1] D.B. Mitzi, O. Gunawan, T.K. Todorov, K. Wang, S. Guha, The path towards a high-performance solution-processed kesterite solar cell, Sol. Energy Mater. Sol. Cells 95 (2011) 1421–1436.
[2] W. Wang, M.T. Winkler, O. Gunawan, T. Gokmen, T.K. Todorov, Y. Zhu, D.B. Mitzi, Device characteristics of CZTSSe thin-film solar cells with 12.6% efficiency, Adv. Energy Mater. 4 (2014) 1301465.
[3] T.K. Todorov, O. Gunawan, T. Gokemn, D.B. Mitzi, Solution-processed $Cu(In,Ga)(S,Se)_2$ absorber yielding a 15.2% efficient solar cell, Prog. Photovolt. Res. Appl. 21 (2013) 82–87.
[4] D.H. Webber, R.L. Brutchey, Alkahest for V_2VI_3 chalcogenides: dissolution of nine bulk semiconductors in a diamine-dithiol solvent mixture, J. Am. Chem. Soc. 135 (2013) 15722–15725.
[5] P.D. Antunez, D.A. Torelli, F. Yang, F.A. Rabu, N.S. Lewis, R.L. Brutchey, Low temperature solution-phase deposition of SnS thin films, Chem. Mater. 26 (2014) 5444–5446.
[6] J.J. Buckley, C.L. McCarthy, J. Del Pilar-Albaladejo, G. Rasul, R.L. Brutchey, Dissolution of Sn, SnO, and SnS in a thiol–amine solvent mixture: insights into the identity of the molecular solutes for solution-processed SnS, Inorg. Chem. 55 (2016) 3175–3180.
[7] D.H. Webber, J.J. Buckley, P.D. Antunez, R.L. Brutchey, Facile dissolution of selenium and tellurium in a thiol–amine solvent mixture under ambient conditions, Chem. Sci. 5 (2014) 2498–2502.

[8] C.L. McCarthy, D.H. Webber, E.C. Schueller, R.L. Brutchey, Solution-phase conversion of bulk metal oxides to metal chalcogenides using a simple thiol-amine solvent mixture, Angew. Chem. Int. Ed. 54 (2015) 1–5.
[9] P. Arnou, C.S. Cooper, A.V. Malkov, J.W. Bowers, J.M. Walls, Solution-processed $CuIn(S,Se)_2$ absorber layers for application in thin film solar cells, Thin Solid Films 582 (2014) 31–34.
[10] P. Arnou, M.F.A. van Hest, C. Cooper, A.V. Malkov, J. Walls, J. Bowers, Hydrazine-free solution deposited $CuIn(S,Se)_2$ solar cells by spray deposition of metal chalcogenides, ACS Appl. Mater. Interfaces 8 (2016) 11893–11897.
[11] D. Zhao, Q. Tian, Z. Zhou, G. Wang, Y. Meng, D. Kou, W. Zhou, S. Wu, Solution-deposited pure selenide ClGSe solar cells from elemental Cu, In, Ga, and Se, J. Mater. Chem. A 3 (2015) 19263–19267.
[12] J. Guo, Y. Pei, Z. Zhou, W. Zhou, D. Kou, S. Wu, Solution-processed $Cu_2ZnSn(S,Se)_4$ thin-film solar cells using elemental Cu, Zn, Sn, S, and Se powders as source, Nanoscale Res. Lett. 10 (2015) 335.
[13] Y. Yang, G. Wang, W. Zhao, Q. Tian, L. Huang, D. Pan, Solution-processed highly efficient $Cu_2ZnSnSe_4$ thin film solar cells by dissolution of elemental Cu, Zn, Sn, and Se powders, Appl. Mater. Interfaces 7 (2015) 460–464.
[14] M. Altosaar, J. Raudoja, K. Timmo, M. Danilson, M. Grossberg, J. Krustok, E. Mellikov, $Cu_2Zn_{1-x}Cd_xSn(Se_{1-y}S_y)_4$ solid solutions as absorber materials for solar cells, Phys. Status Solidi (a) 205 (2008) 167–170.
[15] B. Shin, Y. Zhu, N.A. Bojarczuk, S.J. Chey, S. Guha, Control of an interfacial $MoSe_2$ layer in$Cu_2ZnSnSe_4$ thin film solar cells: 8.9% power conversion efficiency with a TiN diffusion barrier, Appl. Phys. Lett. 101 (2012) 671–673.
[16] X. Zhao, M. Lu, M. Koeper, R. Agrawal, Solution-processed sulfur depleted Cu(In, Ga)Se_2 solar cells synthesized from a monoamine-dithiol solvent mixture, J. Mater. Chem. A 4 (2016) 7390–7397.
[17] J.J. Scragg, T. Ericson, T. Kubart, M. Edoff, C. Platzer-Björkman, Chemical insights into the instability of Cu_2ZnSnS_4 films during annealing, Chem. Mater. 23 (2011) 4625–4633.